

Salt-Free Softening by Thermo-Reversible Ion-Adsorbing Hydrogels

Johannes P. A. Custers,¹ Léon F. S. Stemkens,¹ Rafael Sablong,¹ Dirk T. A. van Asseldonk,¹ Jos T. F. Keurentjes²

¹Afira Water Technologies, De Lismortel 31, 5612 AR Eindhoven, The Netherlands

²Process Development Group, Eindhoven University of Technology, 5600 MB Eindhoven, The Netherlands

Correspondence to: J. P. A. Custers (E-mail: johan.custers@afira.nl)

ABSTRACT: In this article, we demonstrate the properties of a hydrogel capable of adsorbing calcium cations from aqueous streams at ambient temperatures (10–25°C) and showing almost complete desorption of the bound calcium ions at slightly elevated temperatures (40–50°C). Successful breakthrough experiments in a fixed bed column set-up show the potential of the hydrogel in softening water streams from 150 ppm toward <10 ppm hardness levels. The regeneration ability is based on the thermo-reversible internal ion pair-formation mechanism of the hydrogel. Additionally, it was shown that the thermo-reversible adsorption mechanism was successful for magnesium and copper ions too. The exploration of the properties of hydrogel CS-1B14 is the first step in the development of sustainable water-softening processes, both at industrial scale as well as for household applications, using low-grade residual heat to regenerate these gels. In this way, the use of concentrated brine streams, acid/caustic treatment, or high regeneration temperatures is avoided. © 2013 Wiley Periodicals, Inc. *J. Appl. Polym. Sci.* **2014**, *131*, 40216.

KEYWORDS: stimuli-sensitive polymers; polyelectrolytes; adsorption; radical polymerization; gels

Received 26 September 2013; accepted 19 November 2013

DOI: 10.1002/app.40216

INTRODUCTION

Hardness ions like calcium and magnesium cause problems in many processes by forming unwanted salt deposits. For different applications, ranging from household applications like laundry and dish washing to drinking processes, softening of water streams is essential.^{1,2} The current technology to bind multivalent ions is based commonly on the use of ion exchange resins (IEX).^{3,4} Regeneration of IEX typically involves high temperatures^{5–7} or consecutive washing steps involving brine or acid and caustic,⁸ leading to a large amount of waste salt.^{9,10} The disposal of these salts cause salinization of surface waters and soil, which is an increasing burden for the environment. There is upcoming regenerate disposal legislation, where several US states, like California, already installed partial softener bans to deal with salinization of surface waters. As a result, the need for salt free water softening is growing. Therefore, in this article, we focus on a ampholytic hydrogel capable of adsorbing calcium ions from aqueous solutions at room temperature, while the hydrogel can be thermally regenerated at 45°C.

In the last decades, extensive research has been devoted to poly(*N*-isopropylacrylamide) (PNIPAAm)-based hydrogels in order to develop new intelligent materials exploiting its

temperature-dependent volume phase transition.^{11–13} For some applications, there is a focus on multivalent ion adsorption, e.g., for drug delivery,^{14–16} catalyst recycling,¹⁷ removal of specific target ions from aqueous environments,^{18–30} or in the fields of chromatography and sensing.^{31–33} Several attempts have been made to utilize the volume phase transition of PNIPAAm hydrogels to improve the desorption of ions. A few examples have been published in which the lower critical solution temperature (LCST) of PNIPAAm is used as a switch between adsorption and desorption.^{34,35} However, most of these hydrogels deal with ion adsorption at elevated temperatures (40–50°C) and ion desorption at ambient temperature levels (10–20°C). This is not practical for most applications, since multivalent ions often need to be adsorbed from natural water sources, generally found at ambient temperature levels. Furthermore, these hydrogels still show high ion adsorption levels at the desorption temperature, which is unbeneficial in multicyclic adsorption processes.

In this work, an ampholytic hydrogel has been synthesized containing a crosslinked network based on *N*-isopropylacrylamide (NIPAAm) monomers randomly copolymerized with a cationic monomer and a crosslinker *N,N'*-methylenebisacrylamide (MBAAm). Due to the presence of a polyanion in the reaction

Additional Supporting Information may be found in the online version of this article.

© 2013 Wiley Periodicals, Inc.

mixture during the one-pot synthesis, a semi-interpenetrating network (semi-IPN or snake-in-cage)^{36–39} is formed, i.e., a physically entrapped polyanion in a “cage” of positively charged PNIPAAm chains. Because of the presence of PNIPAAm, the hydrogel exhibits an LCST transition. By the incorporation of cationic monomers in the network, the LCST transition is slightly shifted toward higher temperatures, an effect that we counteract by adding a small amount of the more hydrophobic monomer *N*-pentamethylenecrylamide (NPAAm).

EXPERIMENTAL

Hydrogel Composition

The detailed composition of the hydrogel is given in Table I. Hydrogel CS-1B14 consists of the polyanion P(AAmPSS), which contains strongly acidic sulfonate groups, and cationic AAmPTM.Cl monomers, which contain strongly basic quaternary ammonium groups.

Synthesis of NPAAm

Potassium carbonate (200.6 g, Merck) was dissolved into water (580 mL), followed by the addition of piperidine (127 mL, Merck). The solution was cooled in an ice/water bath toward 0°C. Acryloyl chloride (106 mL, Merck) was added drop wise, using a dropping funnel to the mixture, which was mechanically stirred. Thirty minutes after addition, the reaction mixture was heated to 23°C and stirred for 90 min. Next the organic phase with the formed salts was separated from the aqueous phase. The aqueous phase was extracted with dichloromethane (2 × 170 mL, Merck). Next the organic phase was saturated using anhydrous magnesium sulfate (Merck). The hydrated solid was removed by filtration over a glass filter and washed with dichloromethane (2 × 100 mL). Next hydroquinone (0.86 g, Merck) was added to the organic fraction. The volatiles were removed in vacuum using a rotation evaporator. NPAAm was obtained as a colorless liquid after 2 h of distillation of the residual orange liquid under reduced pressure (180°C; distillation temperature: ~75°C). The purity was checked by ¹H-NMR (see Supporting Information section for details of the spectrum).

Synthesis and Analysis of CS-1B14

The gel was prepared by inversed suspension polymerization, with *N*-methylformamide (NMF) as solvent and paraffin oil as the continuous phase. The paraffin oil (ratio oil/NMF = 9.80, volume = 818 mL) was placed in a double-walled reactor of 1 L, which was kept at 24–25°C. Nitrogen gas was bubbled through the oil for 20 h. Next, poly(2-acrylamido-2-methyl-1-propanesulfonic acid (PAAmPSS, 2.29 g, 9.65 mmol), *N*-pentamethylenecrylamide (NPAAm, 6.17 g, 44.3 mmol), 3-acrylamidopropyl trimethyl ammonium chloride (AAmPTM.Cl, 3.05 g, 11.07 mmol), NIPAAm (20.00 g, 177 mmol), and *N,N'*-methyleneacrylamide (1.02 g, 6.62 mmol) were weighed into a 250-mL three-neck flask. *N*-methylformamide (NMF, volume = 83.50 mL) was added and the mixture was stirred at room temperature for 20 h to dissolve all components. The flask was placed in an ice/water bath and the contents were placed under an inert atmosphere by three successive vacuum/N₂ cycles in 20 min. Ammonium persulfate (APS, 250 mg, 1.096 mmol) was added. After complete dissolution, the mixture was transferred

Table I. Composition^a of Hydrogel CS-1B14 in mol. eq.

NIPAAm	0.80
NPAAm	0.20
MBAAm ^b	0.03
P(AAmPSS) ^{b,c,d}	0.05
AAmPTM.Cl ^{b,c}	0.05
Solvent	NMF
Continuous phase	Paraffin oil
Total monomer concentration in solvent /mol.L	3.0

^a Structural formulas are given in the Supporting Information.

^b Based on amount of NIPAAm + NPAAm.

^c With P(AAmPSS) as poly(2-acrylamido-2-methyl-1-propanesulfonic acid and AAmPTM.Cl as 3-acrylamidopropyl trimethyl ammonium chloride.

^d Value based on monomer AAmPSS.

to the reactor via syringe in 10 min. The mixture was stirred at 175 rpm. After complete addition of *N,N,N',N'*-tetramethylenediamine (TMEDA, 0.83 mL, 5.54 mmol), the suspension was stirred at 175 rpm for 2 h and 45 min. After stirring for 30 min, another batch of TMEDA (0.83 mL, 5.54 mmol) was added. The formed beads were isolated after 2 h and 45 min, by filtration over a 250-micron sieve. The beads were swirled in hexane (100 mL) for 5 min and filtered. This was repeated twice. The beads were stirred in a 1M NaOH solution (200 mL). After filtration the beads were soaked into 250 mL water at least three times for a couple of hours and analyzed with FT-IR. The dry particle size range (0.20–0.66 mm) and the average particle size (0.39 mm) was estimated by a Dino-Lite AM4013TL premier digital microscope.

FT-IR Analysis

Gel CS-1B14 was analyzed by an Avatar 330 FT-IR spectrometer. The following absorption peaks were identified from the spectrum, which is given in the Supporting Information section:

3285 cm⁻¹ (sec. amine, NH stretch), 2970 cm⁻¹ (isopropyl, CH stretch), 2931 cm⁻¹ (methylene, CH stretch), 1634 cm⁻¹ (CO amide stretch), 1538 cm⁻¹ (NH bend), 1456 cm⁻¹ (methylene, CH₂ bend), 1366 cm⁻¹ (SO₃H), 1190 cm⁻¹ (CN stretch), 1172 cm⁻¹ (SO₃H stretch) and 1038 cm⁻¹ (SO stretch)

Batch Adsorption Experiments

In order to determine the amount of calcium, magnesium or copper adsorbed by the hydrogel, dry hydrogel (250 mg) was put into a CaCl₂, MgCl₂, or CuCl₂ solution (25 mL) of a specific concentration adding NaCl up to an IS of 0.02 mol L⁻¹. The solution, containing the hydrogel, was kept at the desired temperature for 2 days to equilibrate. Next, samples (10 mL) were taken from the solution outside the gel and calcium, magnesium, and copper were analyzed by colorimetric titration with ethylenediaminetetraacetic acid (EDTA).⁴⁰ The adsorbed amount was calculated from the difference of the measured concentration with the initial total concentration, corrected for the concentration of free divalent cations inside the hydrogel network. For this correction, it was assumed that the free concentration divalent cations equals the concentration divalent cations outside the gel. The swelling of the gels was measured at

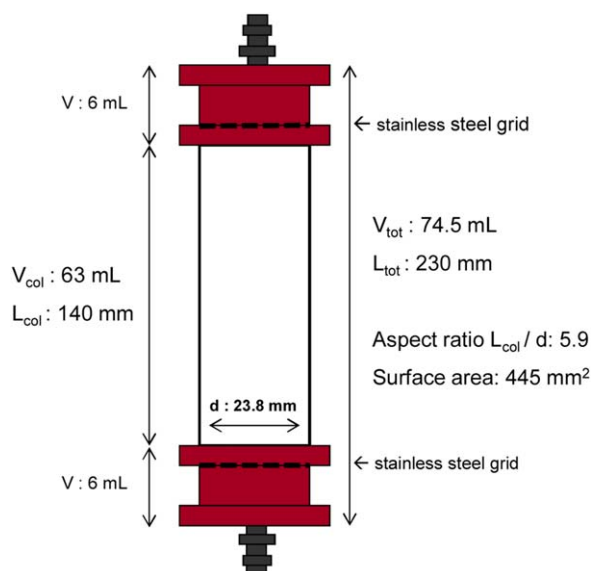


Figure 1. Column geometrics. [Color figure can be viewed in the online issue, which is available at wileyonlinelibrary.com.]

all temperatures by weighing the swollen gels on a mass balance.

Isotherms were constructed from the adsorption values. These isotherms were fitted using the Langmuir model to obtain the maximum adsorption capacity S and the affinity constant K , which is a well-known procedure that is described elsewhere.^{22,27}

Breakthrough Curve Experiments

For the determination of the breakthrough curves a 63 mL column was used (Figure 1) containing 10 g CS-1B14 gel. In swollen state the gel occupies the whole volume, resulting in a bed volume of 63 mL.

The column was placed vertically and connected to a Watson Marlow 505S tubing pump, which was operating down-top at a setting of 1.5 rpm during the experiment. Before each experiment, the gel in the column was brought in equilibrium with a 45°C feed solution, which contained 60, 90, or 150 ppm calcium (depending on the experiment) adjusted to a ionic strength of 0.02M using NaCl as a background electrolyte. The column was equilibrated by pumping the feed solution through the column at 45°C and taking 10 mL samples at the exit of the column. The equilibrium point was taken as the situation when the concentration calcium in the exit samples equaled the concentration calcium that entered the column. The situation obtained after drainage of the column by gravity is the starting point for adsorption experiments and was considered to be the regenerated state of the gel.

The adsorption is carried out by filling the column with a feed solution (60, 90, or 150 ppm calcium) at room temperature, in 20 min, in order to be sure to get the gel from a shrunken to a fully swollen state. Next, the feed solution was pumped continuously through the column (1.5 rpm) and samples of 10 mL were collected at the exit of the column, which were analyzed for the calcium concentration by colorimetric titration. An

outlet concentration of 20 ppm Ca^{2+} was considered to be the breakpoint. Immediately after the adsorption step, the regeneration step was carried out by placing the entire disconnected column, with closed inlet and outlet, in an oven at 45°C for 30 min, followed by a drainage. The liquid from the drained column was analyzed for calcium. After that, the column was connected again to the pump and 18 mL 45°C feed solution, having similar concentration as the feed solution during the adsorption step, was fed to the column in such a way that the shrunken gel bed was completely immersed into liquid. The column was closed on both the sides, disconnected again and placed in the oven for about 1 h to keep the temperature at 45°C. Finally, the column was drained again and the resulting water was analyzed for calcium.

RESULTS AND DISCUSSION

In order to demonstrate the unique property of the gel, we have taken calcium ions as the main target in this paper, because it is the most common divalent ion to be removed from aqueous streams (e.g. in softening applications). The property was tested for Cu^{2+} and Mg^{2+} ions as well and corresponding equilibrium adsorption results are mentioned in this article too. Experiments involving Fe^{2+} and Fe^{3+} ions were unsuccessful as no reliable adsorption data could be retrieved from those experiments, mainly due to oxidation effects. The formation of iron oxides caused a red-brownish discoloration of the hydrogel spheres.

Batch Adsorption and Swelling Experiments

The adsorption of calcium ions and the swelling ratio of the gel as a function of temperature at varying calcium concentrations are given in Figure 2(a,b). A clear step-change transition can be seen in the LCST trajectory (between 30 and 40°C), when the calcium adsorption by the hydrogel strongly decreases with increasing temperature. This is caused by the volume phase transition of the PNIPAAm (around 33°C), as will be outlined in more detail below. As a result of the reversibility of this phase transition, the adsorption-desorption behavior of these gels is completely reversible, thereby following the curves of Figure 2a. Furthermore, a decreasing swelling ratio ($\text{SR} = \text{mass swollen gel} / \text{mass dry gel}$) with temperature is observed (Figure 2b), which can be attributed to the decreasing solubility of PNIPAAm with temperature. In the swollen hydrogel, free ions are accompanying the absorbed water. Consequently, the calcium adsorption values should be corrected for the concentration free calcium ions inside the hydrogel network, which are, therefore, subtracted from the total absorption values. For this correction, it was assumed that the free concentration calcium equals the concentration calcium outside the gel. This correction rules out the possibility to assign the adsorption effect to the differences in swelling at different temperatures. The corrected values are displayed in Figure 2a.

The reversible ion-binding mechanism of these gels is illustrated in Figure 3, where we hypothesize that the mechanism can be allocated to the change in local charge density of the cationic groups inside the gel as a function of temperature. There is an equal amount of anionic and cationic charged groups in the hydrogel, so macroscopically it is neutral. However, at low

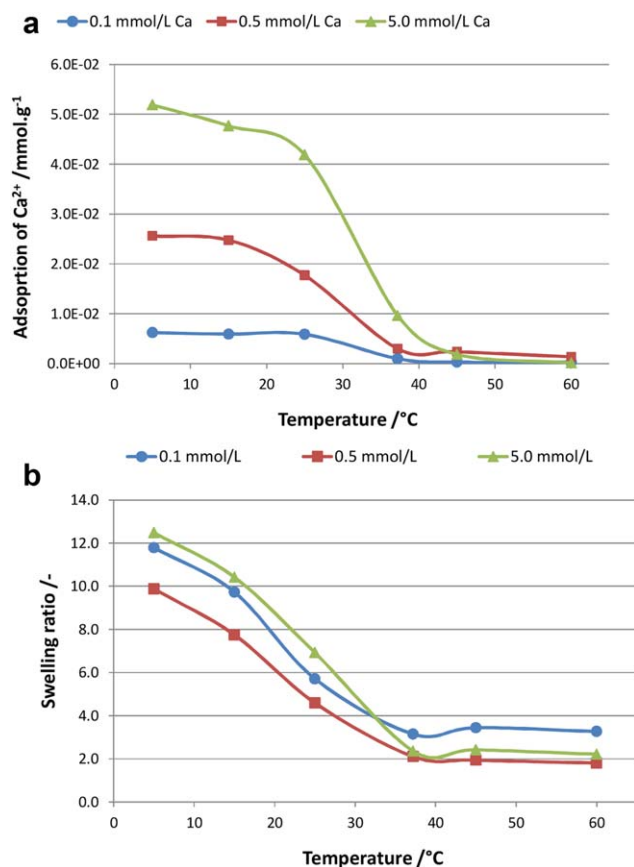


Figure 2. (a) Equilibrium adsorption–temperature curves of Ca²⁺ at different calcium chloride concentrations. In these experiments, the ionic strength was kept constant at 0.02 mol L⁻¹ using sodium chloride as a background salt. Adsorption values are corrected for free calcium ions due to swelling (b). Equilibrium swelling–temperature curves of Ca²⁺ at different calcium chloride concentrations. [Color figure can be viewed in the online issue, which is available at wileyonlinelibrary.com.]

temperatures, i.e., below LCST, the hydrogel acts as a hydrophilic entity and will swell. Solution ions like Ca²⁺ and chloride Cl⁻ are able to move freely into the gel.

The charged groups of the polyanion in the hydrogel are situated very closely to each other, because they exist as neighboring monomers in a single polymer chain. At nonacidic pH levels (pH > pK_a), these charged groups generate an electrostatic potential that allows the solution calcium ions to adsorb to the polyanion. Conversely, the randomly distributed cationic monomers in the network are as far apart as possible because of the entropic nature of the hydrophilic chains (these want to dissolve). At swelling conditions, they possess a significantly lower local charge density, which leads to a much lower electrostatic contribution as compared to the anionic part.

At temperatures above the LCST, typically >40°C, the situation changes. The PNIPAAm part of the hydrogel becomes hydrophobic and the hydrogel tends to shrink and expels some of the absorbed liquid. This shrinking behavior most likely leads to an increase in internal ion pair formation between the anionic groups of the entangled polyanion and the copolymerized

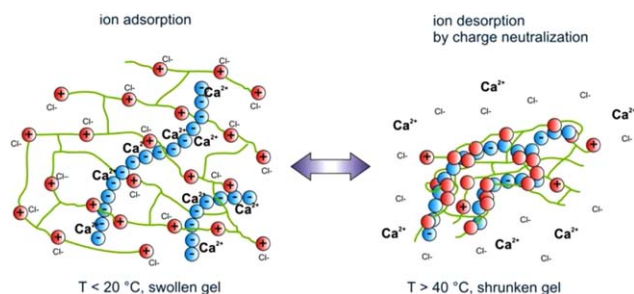


Figure 3. Schematic representation of the thermo-reversible ion-binding mechanism. For clarity reasons, the noncharged NIPAAm and NPAAm monomers are presented as green solid lines. [Color figure can be viewed in the online issue, which is available at wileyonlinelibrary.com.]

cationic monomers of the PNIPAAm matrix. This is most likely due to the fact that the local density of cationic groups is much higher in the shrunken state than in the swollen state, whereas the closest distance between two anionic groups hardly changes during this volume phase transition. Consequently, the electrostatic attraction between the oppositely charged groups increases, thereby favoring the formation of internal ion pairs, releasing the smaller adsorbed ions to the solution.

The unique property of hydrogel CS-1B14 was not encountered before in literature. It is known that for PNIPAAm-based hydrogels copolymerized with solely anionic groups the opposite behavior is found, a shrinking hydrogel leads to an increase in adsorption for solution cations, because the macroscopic density of anionic groups is higher in the shrunken gel state.^{41,42} A similar effect is found for ampholytic hydrogels having both their cationic and anionic charged groups randomly copolymerized in the network. Furthermore, we have not observed any calcium adsorption with noncharged PNIPAAm hydrogels in the full temperature range 10–80°C. Moreover, in contrast with traditional demineralization resins, which need demineralized water to regenerate,³² the gels described here can effectively be

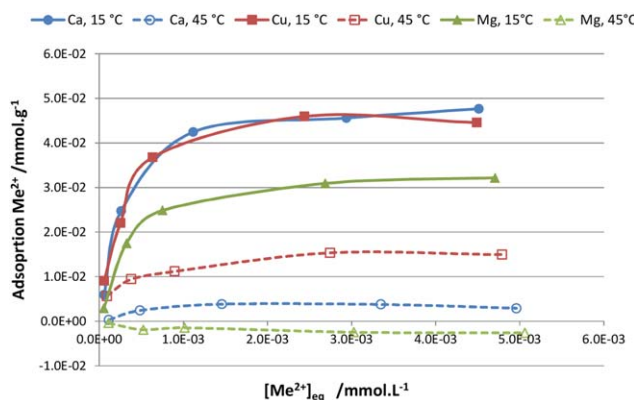


Figure 4. Adsorption isotherms for Ca²⁺, Cu²⁺, and Mg²⁺ adsorption onto gel CS-1B14. In these experiments, the ionic strength was kept constant at 0.02 mol L⁻¹ using sodium chloride as a background salt. Adsorption values are corrected for free divalent ions due to swelling. The divalent ion is indicated with the symbol Me²⁺. [Color figure can be viewed in the online issue, which is available at wileyonlinelibrary.com.]

Table II. Langmuir Parameters for the Adsorption Isotherms of CS-1B14

Isotherm	Max. capacity, S (mmol g ⁻¹)	Affinity constant, K (L mol ⁻¹)	R^2
Ca ²⁺ , 15°C	5.10 E -02	3051	0.9983
Ca ²⁺ , 45°C	3.48 E -03	2624	0.9163
Cu ²⁺ , 15°C	4.75 E -02	4584	0.9978
Cu ²⁺ , 45°C	1.58 E -02	4242	0.9969
Mg ²⁺ , 15°C	3.54 E -02	2362	0.9961
Mg ²⁺ , 45°C ^a	-	-	-

^aThe isotherm for Mg²⁺ at 45°C could not be fitted adequately by the Langmuir model, because of the negative adsorption values as shown in Figure 4.

regenerated at moderate ionic strengths (including feed solution water conditions), which clearly is an advantage.

Although calcium ions are the primary target in this paper it is still very useful and interesting to test this hydrogel property with other divalent ions, like magnesium and copper. Therefore, adsorption isotherms were constructed for gel CS-1B14 in CaCl₂, MgCl₂, and CuCl₂ solutions at temperatures of 15°C and 45°C. The results are depicted in Figure 4. In addition, the isotherms were fitted with the Langmuir model in order to obtain values for the maximum adsorption capacity S and affinity constant K . The results for the fitting parameters S and K are tabulated for the six isotherms in Table II.

Note that the slightly negative adsorption values for Mg²⁺ at 45°C in Figure 4 can be physically interpreted as the situation where the (initially dry) hydrogel absorbed some water, but effectively expels all Mg²⁺ ions leading to a small increase in Mg²⁺ concentration outside the gel.

It clearly can be observed from Figure 4 that for all three divalent cations there is a large difference in adsorption between the temperatures 15°C and 45°C, which indicates that the thermo-reversible mechanism works for Mg²⁺ and Cu²⁺ too. When comparing the S and K values from Table II between 15°C and 45°C for the three cations, we may observe a large decrease in the value for the maximum capacity S , but hardly any decrease in the value for affinity constant K . From this result, one may cautiously conclude that the thermo-reversible adsorption mechanism of the hydrogel is mainly a difference in the availability of adsorption sites between the two temperatures. This conclusion matches our hypothesis, as stated earlier, that the mechanism is due to a difference in the degree of internal ion pair formation.

Furthermore, Figure 4 shows that the adsorption difference between 15°C and 45°C is highest for calcium, followed by magnesium and copper. It is not immediately obvious what effects mainly determine this difference, as it will be a complex interplay between affinity, steric effects, ion hydration effects, ion size, and electrostatic repulsion. It seems, however, that the adsorption values at 45°C show a similar trend as the corresponding value of the affinity constant K (using the assumption that magnesium has lower affinity than calcium, which seems fair because of its negative adsorption values).

In general, a typical softening process uses a fixed bed column and consists of an adsorption and regeneration step.⁴³ Following a similar process, in the adsorption step a feed solution, containing calcium, is led through a column at 20°C until the breakpoint is reached, which is followed by a regeneration step using water of 45°C. To demonstrate the softening capability of the hydrogel, breakthrough curves were determined for 60, 90, and 150 ppm Ca²⁺ feed solutions. For these experiments, a 63-mL column was filled with 10 g of CS-1B14 gel, which was initially in an equilibrium state with the feed solution of 45°C. In this equilibrium state at 45°C the gel is not totally empty, as can be seen in Figure 2a, which automatically implies that a very small amount of calcium already is present in the gel at the start of the adsorption experiment.

The graph in Figure 5 shows the adsorption breakthrough curves for 60, 90, and 150 ppm Ca²⁺ solutions, adjusted to an ionic strength of 0.02M using sodium chloride as a background electrolyte. It can clearly be seen that all three feed solutions can be softened to a hardness level lower than 10 ppm Ca²⁺. Generally, water with a hardness level <20 ppm is considered being soft water. From the 150 ppm curve, an adsorption capacity of 0.05 mmol/g dry weight was calculated, which closely matches the values found in the batch experiments of Figure 2a. The measured CS-1B14 capacity (see also Table II) is about 5% of the ion exchange capacity level of commercial resins,⁴³ which is not a competitive value yet. However, the interesting property of this resin is that it may be fully regenerated by low-grade heat of 45°C, where no extra chemicals are needed for regeneration.

The regeneration step was carried out by heating the column and its contents indirectly (e.g. by heat exchange or by electricity) to a temperature of 45°C. The gel shrinks and the water surrounding the gel, containing a very high calcium concentration, is drained from the column. In this way, already 80–85% of the adsorbed calcium ions is removed from the gel. An additional flush with 10–15 mL of heated water (45°C, 60, 90, or

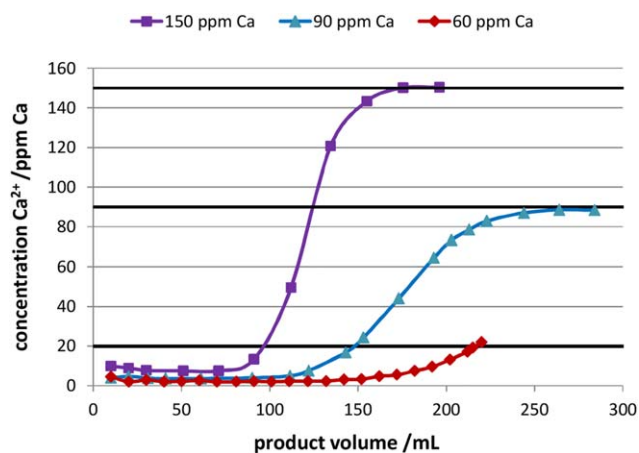


Figure 5. Breakthrough curves of gel CS-1B14 for three different hardness levels, i.e., 60, 90, and 150 ppm Ca²⁺. The adsorption temperature was 20°C and the initial state of the gel was a gel equilibrated against a 45°C feed solution. [Color figure can be viewed in the online issue, which is available at wileyonlinelibrary.com.]

150 ppm water), results in an additional removal of the remaining 15–20% amount of calcium from the gel. Following this procedure, the gel has returned to the initial state prior to the adsorption step, which is equal to the equilibrium state with a 45°C feed solution. As the bed volume is defined as the column volume occupied by the swollen gel, a total water volume of about 1.2 bed volumes is needed for regeneration, which is much less than the typical three bed volumes needed for conventional IEX processes.⁴³

Although many aspects of the gel still have to be investigated, like kinetics, multi-cycle lifetime and fouling risk, the resin as presented here already shows its potential. In order to have an economically feasible resin, the ion adsorbing capacity of gel CS-1B14 needs to increase. At the moment, the theoretical built-in capacity for calcium (equal to half the amount of anionic groups) of gel CS-1B14 is about 0.2 mmol Ca²⁺ per gram dry gel, which indicates that 75% of the anionic groups are still inactive for adsorption. Most likely, this is due to irreversible ion pair formation, caused by the spatial inhomogeneity of the hydrogel introduced by the current synthesis procedure.^{44–46} We are confident that reduction of the ion pair formation degree and the gel inhomogeneity will lead to the necessary improvements in the near future.

CONCLUSIONS

In summary, PNIPAAm-based ampholytic semi-IPN hydrogels are presented that use their temperature-responsive volume phase transition as a switch between adsorption and desorption of calcium, magnesium, and copper cations from aqueous solutions. Equilibrium adsorption values, swelling ratios, and breakthrough curves have demonstrated the features of hydrogel CS-1B14. Results indicate that the thermo-reversible effect is most likely due to an increase in internal ion pair formation degree with increasing temperature. Knowing that the volume phase transition takes place at temperatures between 30 and 40°C, these hydrogels open up a new route to the development of materials that have the potential to be used in many ion removal applications, where low grade residual heat is available to regenerate the hydrogel thermally, which avoids the disposal of large salty waste streams to the environment.

ACKNOWLEDGMENTS

The authors acknowledge the Dutch governmental organization NL Agency for financial support.

REFERENCES

1. Boerlage, S. F. E.; Kennedy, M. D.; Bremere, I.; Witkamp, G. J.; Van der Hoek, J. P.; Schippers, J. C. J. *J. Membr. Sci.* **2002**, *197*, 251.
2. Bonne, P. A. C.; Hofman, J. A. M.; Van der Hoek, J. P. *Desalination* **2000**, *132*, 109.
3. Abrams, I. M.; Millar, J. R. *React. Funct. Polym.* **1997**, *1–2*, 7.
4. Colela, C. *Mineralium Deposita*. **1996**, *6*, 554.
5. Khamizov, R. A.; Ivanov, V. A.; Madani, A. A. *React. Funct. Polym.* **2010**, *70*, 521.
6. Chanda, M.; Pillay, S. A.; Sarkar, A.; Modak, J. M. *J. Appl. Polym. Sci.* **2009**, *111*, 2741.
7. Bolto, B. A.; Eppinger, K. H.; Jackson, M. B.; Siudak, R. V. *Desalination* **1980**, *34*, 171.
8. Alexandratos, S. D. *Ind. Eng. Chem. Res.* **2009**, *48*, 388.
9. Small, H.; Stevens, T. S.; Bauman, W. C. *Anal. Chem.* **1975**, *47*, 1801.
10. Flodman, H. R.; Dvorak, B. I. *Water Environ. Res.* **2012**, *84*, 535.
11. Nayak, S.; Lyon L. A. *Angew. Chem. Int. Ed.* **2005**, *44*, 7686.
12. Kirsebom, H.; Galaev, I. Y.; Mattiasson, B. *J. Polym. Sci. Part B: Polym. Phys.* **2011**, *49*, 173.
13. Chaterji, S.; Kwon, I. K.; Park, K. *Prog. Polym. Sci.* **2007**, *32*, 1083.
14. Byrne, M. E.; Park, K.; Peppas, N. *Adv. Drug Delivery Rev.* **2002**, *54*, 149.
15. Funueanu, G.; Constantin, M.; Oanea, I.; Harabagiu, V.; Ascenzi, P.; Simionescu, B. C. *Biomaterials* **2010**, *31*, 9544.
16. Lin, C.-C.; Metters, A. T. *Adv. Drug Delivery Rev.* **2006**, *58*, 1379.
17. Barbaro, P.; Liguori, F. *Chem. Rev.* **2009**, *109*, 515.
18. Mizoguchi, K.; Ida, J.; Matsuyama, T.; Yamamoto, H. *Sep. Purif. Technol.* **2010**, *75*, 69.
19. Tokuyama, H.; Kanehara, A. *React. Funct. Polym.* **2007**, *67*, 136.
20. Tokuyama, H.; Ishihara, N. *React. Funct. Polym.* **2010**, *70*, 610.
21. Barati, A.; Asgar, M.; Miri, T.; Eskandari, Z. *Environ. Sci. Res.* **2013**, *20*, 6242.
22. Huang, D.; Wang, W.; Wang, A. *Adsorpt. Sci. Technol.* **2013**, *31*, 611.
23. Wang, J.; Li, X. *Ind. Eng. Chem. Res.* **2013**, *52*, 572.
24. Kaviani, I.; Plieger, P. G.; Kandile, N. G.; Harding, D. R. *Carbohydr. Polym.* **2012**, *87*, 881.
25. Fei, C.; Huang, D.; Feng, S. *J. Polym. Res.* **2012**, *19*, 9929.
26. Özkahraman, B.; Acar, I.; Emik, S. *Clean Soil, Air, Water* **2011**, *39*, 658.
27. Singh, T.; Singhal, R. *J. Appl. Polym. Sci.* **2012**, *125*, 1267.
28. Yan, H.; Dai, J.; Yang, Z.; Yang, H.; Cheng, R. *Chem. Eng. J.* **2011**, *174*, 586.
29. Guilherme, M. R.; Reis, A. V.; Paulino, A. T.; Moia, T. A.; Mattoso, L. H. C.; Tambourgi, E. B. *J. Appl. Polym. Sci.* **2010**, *117*, 3146.
30. Carvalho, H. W. P.; Batista, A. P. L.; Hammer, P.; Luz, G. H. P.; Ramalho, T. C. *Environ. Chem. Lett.* **2010**, *8*, 343.
31. Byrne, M. E.; Salián, V. *Int. J. Pharm.* **2008**, *364*, 188.
32. Alexander, C.; Andersson, H. S.; Andersson, L. I.; Ansell, R. J.; Kirsch, N.; Nicholls, I. A.; O'Mahony, J.; Whitcombe, M. *J. J. Mol. Recognit.* **2006**, *19*, 106.
33. Marty, J. D.; Mauzac, M. *Adv. Polym. Sci.* **2005**, *172*, 1.
34. Yamashita, K.; Nishimura, T.; Ohashi, K.; Ohkouchi, H.; Nango, M. *Polym. J.* **2003**, *35*, 545.

35. Alvarez-Lorenzo, C.; Hiratani, H.; Tanaka, K.; Stancil, K.; Grosberg, A. Y.; Tanaka, T. *Langmuir* **2001**, *17*, 3616.
36. Hatch, M. J.; Dillon, J. A.; Smith, H. B.; *Ind. Eng. Chem.* **1957**, *49*, 1812.
37. Lesslauer, W.; Lauger, P. *J. Phys. Chem.* **1967**, *71*, 2544.
38. Murali Mohan, Y.; Geckeler, K. E. *React. Funct. Polym.* **2007**, *67*, 144.
39. Qu, R.; Sun, Y.; Wang, C.; Lu, S.; Yu, H.; Cheng, G. *J. Appl. Polym. Sci.* **2002**, *84*, 310.
40. Pollard, F. H.; Martin, J. V. *Analyst* **1956**, *81*, 348.
41. Alvarez-Lorenzo, C.; Guney, O.; Oya, T.; Sakai, Y.; Kabayashi, M.; Enoki, T.; Takeoka, Y.; Ishibashi, T.; Kuroda, K.; Tanaka, K.; Wang, G.; Grosberg, A. Y. *J. Chem. Phys.* **2001**, *114*, 2812.
42. D'Oleo, R.; Alvarez-Lorenzo, C.; Sun, G. *Macromolecules* **2001**, *34*, 4965.
43. Zagorodni, A. A. *Ion Exchange Materials, Properties and Applications*, Elsevier: Oxford; **2007**, p 78.
44. Liu, R.; Oppermann, W. *Macromolecules* **2006**, *39*, 4159.
45. Nie, J.; Du, B.; Oppermann, W. *Macromolecules* **2004**, *37*, 6558.
46. Suzuki, T.; Karino, T.; Ikkai, F.; Shibayama, M. *Macromolecules* **2008**, *41*, 9882.